arXiv:astro-ph/0011337v1 17 Nov 2000

Observation of X-ray lines from a Gamma-Ray Burst (GRB991216): Evidence of Moving Ejecta from the Progenitor

L. Piro[*], *G. Garmire* [†], *M. Garcia*[‡], *G. Stratta*[*], *E. Costa*[*], *M. Feroci*[*], *P. Mészáros*[†], *M. Vietri*[+], *H. Bradt*[1], *D. Frail*[2], *F. Frontera*[3], *J. Halpern*[4], *J. Heise*[5], *K. Hurley*[6], *N. Kawai*[7], *R. M. Kippen*[8], *F. Marshall*[9], *T. Murakami*[10], *V. V. Sokolov*[11], *T. Takeshima*[12], *A. Yoshida*[7]

[*] Istituto Astrofisica Spaziale, C.N.R., Via Fosso del Cavaliere, 00133 Roma, Italy [†] Department of Astronomy and Astrophysics, 525 Davey Lab, Penn State University, University Park, PA 16802, USA [‡] Center for Astrophysics, Harvard-Smithsonian, 60 Garden St. Cambridge, MA 02138, USA [+] Department of Physics, Universita' Roma Tre, Via della Vasca Navale 84, 00146 Roma, Italy [1] MIT, 77 Massachusetts Avenue, Cambridge, MA 02139-4307, USA [2] NRAO, 1003 Lopezville Rd., Socorro, NM 87801, USA [3] ITeSRE/C.N.R., Via Gobetti 101, 40129 Bologna, Italy [4] Columbia University, Dept. of Astrophysics, 545 W. 114th St., New York, NY 10027, USA [5] Space Research Organization in the Netherlands, Sorbonnelaan 2, 3584 CA, Utrecht, The Netherlands [6] UC Space Science Laboratory, Berkeley, CA 94720-7450, USA [7] RIKEN, 2-1 Hirosawa, Wako-Shi, Saitama 351-0198, Japan [8] University of Alabama, NASA/MSFC, Huntsville, AL 35899, USA [9] NASA/GSFC, Code 661, Greenbelt, Maryland 20771, USA [10] ISAS, 3-1-1 Yoshinodai, Sagamihara, Kanagawa 229-8510, Japan [11] SAO/RAS, Special Astrophysical Observatory Nizhnij Arkhyz, Zelenchukskaya, Karachaevo-Cherkesia, Russia 369167 [12] NASDA, National Space Development Agency of Japan, WTC Building 2-4-1, Hamamatsu-cho Minato-ku, Tokyo, 105-60 Japan

published in Science, 290, 955 (2000)

We report on the discovery of two emission features observed in the X-ray spectrum of the afterglow of the gamma-ray burst (GRB) of 16 Dec. 1999 by the Chandra X-Ray Observatory. These features are identified with the Ly$_\alpha$ line and the narrow recombination continuum by hydrogenic ions of iron at a redshift $z = 1.00 \pm 0.02$, providing an unambiguous measurement of the distance of a GRB. Line width and intensity imply that the progenitor of the GRB was a massive star system that ejected, before the GRB event, $\approx 0.01 M_\odot$ of iron at a velocity $\approx 0.1c$, probably by a supernova explosion.

The nature of the progenitors of GRB's is an unsettled issue of extreme importance [1]. The merging of a binary system of compact objects (such as black holes, neutron stars, and white dwarfs) or the collapse of a massive star (hypernova or collapsar) could all deliver the energy required by a GRB, but observational evidence discriminating against the various models is still missing. This evidence can be gathered through the measurement of lines produced by the medium surrounding the GRB [2, 3, 4]. However, while observations of GRB afterglows have provided much information on the broad band spectral continuum and its origin [5, 6], they have not yet given results of comparable importance on spectral lines. In the optical range current measurements are inconclusive, because all of the spectral emission lines observed so far are produced by the host galaxy rather than at the burst site. The x-ray range appears more promising because theoretical computations show that only a dense, massive medium close to the GRB site - such as that expected in the case of a massive progenitor - could produce an iron emission line detectable with current x-ray instrumentation [7-10]. Indeed, marginal evidence of iron features has been claimed in two x-ray afterglows [11, 12] but the case is still controversial not only for the limited statistical weight, but also for the tight upper limits measured in other afterglows [13], and for the claimed inconsistency between the redshift derived for GB970828 in x-rays and from the host galaxy [14], that could be reconciled only assuming different physical conditions in the two bursts [9]. The prospect of gathering unique data on the nature of the progenitor

made the search for spectral features one of the primary objectives of a Chandra [15] GRB observation program.

The first Chandra observation of a GRB was performed on the event of 16 Dec. 1999, one of the brightest GRB ever detected by the Burst And Transient Source Experiment (BATSE) on board of the Compton Gamma-Ray Observatory, with fluence $S_\gamma > 2.5 \times 10^{-4}$ erg cm^{-2} above 20 keV [16]. Following the localization of a strong x-ray afterglow by Rossi X-ray Transient Explorer (guided by the rapid BATSE GRB localization) and the characterization of its temporal behaviour [17], and a confirming localization by the interplanetary network [18], we estimated that the X-ray flux would only decay to $\approx 10^{-12}$erg cm^{-2} s^{-1} by the time Chandra could be re-oriented to point at it. This flux level is high enough to employ the gratings in conjunction with the Advanced CCD Imaging Spectrometer in the Spectroscopic configuration (ACIS-S), and we selected this instrument configuration for the observation. Chandra acquired the target on 18 Dec., 04:38 U.T., i.e. 37 hours after the GRB, and observed it for 3.4 hours. We found a bright x-ray source [19] with a position (right ascension (2000) = $05^h09^m31^s.35$, declination (2000) = $11°17'05''.7$) coincident within the 1.5" error with the optical [20] and radio [21] transients and with a flux consistent with that expected from the XTE extrapolation.

The spectrum of the x-ray afterglow (Fig. 1) shows an emission line at energy $E = 3.49 \pm 0.06$ keV. Due to the ubiquity and prominence of iron lines in astrophysical objects [22] we argue that this line is associated with emission from iron. Some ambiguity remains in the rest energy of the emission. Iron K_α lines have rest energies ranging from 6.4 keV (fluorescence of neutral atoms) to 6.7 keV (He-like ions) or 6.97 keV (H-like ions). In those three cases we would obtain redshifts of $z = 0.83 \pm 0.02$, $z = 0.92 \pm 0.02$ and $z = 1.00 \pm 0.02$, respectively. In particular, at higher energies the ACIS-S spectrum shows evidence of a recombination edge in emission at $E = 4.4 \pm 0.5$ keV. Identifying this feature with the iron recombination edge with rest energy of 9.28 keV gives $z = 1.11 \pm 0.11$, consistent with the highest of the redshifts implied by the emission line.

An iron recombination edge at 9.28 keV is indeed expected when the iron emission is driven by photoionization and the medium is heavily ionized by the radiation produced by the GRB and its afterglow [2, 9, 23]. If the medium lies in the line of sight, the edge is expected to be seen in absorption at early times [3, 9], and evidence of such a feature has been found in another GRB [24]. At later times, when the medium becomes heavily ionized and recombination takes place, the edge is seen in emission. This is our case. In this condition x-ray lines are produced almost exclusively through recombination of electrons on H-like iron [25]. The measured intensities of the two features are also consistent with theoretical expectations ($I_{edge}/I_L \approx 0.93(kT/keV)^{0.2}$ [23], where I_{edge} and I_L are the intensities of the recombination edge and emission lines, respectively, and T is the electron temperature of the gas). We therefore conclude that the redshift of the GRB is $z = 1.00 \pm 0.02$. We stress that this measurement is consistent with the most distant absorption system (z=1.02) found in the line of sight towards GRB991216 by optical spectroscopy [26]. This system should then be in the host galaxy of the GRB, which has probably been identified in deep optical images [27].

The detection of the line, the measurement of the distance ($D = 4.7\ Gpc$, assuming $H_0 = 75 km\ s^{-1} Mpc^{-1}$ and $q_0 = 0.5$) and the fact that the driving process is recombination allow us to derive a lower limit on the mass of the line emitting medium. The number of iron atoms N_{Fe} needed to produce the observed photon line luminosity[1] $L = 10^{52} L_{52} = 8 \times 10^{52}\ photons\ s^{-1}$ is $N_{Fe} = L_L t_{rec}$, where each of the N_{Fe} iron atom produces t_{rec}^{-1} line photons per second. The recombination time of iron [2] is $t_{rec} = 30 T_7^{1/2} n_{10}^{-1}\ s$, where $T = 10^7 T_7 K$ and $n = 10^{10} n_{10} cm^{-3}$ are respectively the temperature and density of the electrons. The temperature is constrained from the width of the recombination edge to be $kT > 1$ keV, therefore implying $t_{rec} > 30 n_{10}^{-1} s$. The total mass of material in the line region can be written

$$M = M_{Fe}/(X_{Fe} 1.8 \times 10^{-3}) > 7 X_{Fe}^{-1} L_{52} n_{10}^{-1} M_\odot \quad (1).$$

[1] hereafter some quantities are expressed as $Y = Y_n \times 10^n$

X_{Fe} is the iron abundance relative to the sun, where the iron is a fraction 1.8×10^{-3} of the total mass. The requirement that the ionization parameter ξ be high enough to keep the Fe in a H-like state, i.e. $\xi = 4\pi D^2 F_x / nR^2 > 10^4$ [25], allows us to estimate $n_{10} < 15$ where we have used the flux observed by Chandra of $F_X = 2.3 \times 10^{-12}$erg cm^{-2} s^{-1} and assumed that the distance of the gas from the GRB is $R > 2 \times 10^{15}$cm. The latter condition derives from the presence of the line 1.5 days after the GRB which, in the cosmological rest frame of the burst, is $(1+z)^{-1}$ times shorter than observed. Using this limit on the density and the observed line luminosity allows us to set a lower limit on the mass of:

$$M \gtrsim 5 X_{Fe}^{-1} M_\odot;\ M_{Fe} \gtrsim 0.01 M_\odot$$

This large mass is not ejected during the GRB explosion, but in an earlier phase. This is the only possible condition to have the material moving at subrelativistic speed (as shown below) and be illuminated by GRB photons. The large mass of pre-ejected material excludes progenitor models based on double neutron stars, black hole - neutron star and black hole - white dwarf. These systems eject material long before they actually merge and the progenitors of these GRB travel far from their formation sites (and their ejecta) before producing GRB [1]. Conversely, massive progenitors - which evolve more rapidly - lead to a GRB in a mass-rich environment.

Additional information on the origin of the ejecta is derived from the line width ($\sigma_L = 0.23 \pm 0.07$ keV, Fig.1). Thermal broadening ($\Delta E/E = (kT/Am_pc^2)^{1/2}$) is negligible here, while Compton broadening would require a Thompson optical depth $\tau > 1$, which is excluded by [3]. The line width is therefore kinematical, with $v \approx 0.1c$. Normal winds from stars are not compatible with the parameters of the medium. In fact, the wind density is $n \approx 10^3 (\dot{M}_{-4} R_{16}^{-2} (v/0.1c)^{-1} cm^{-3}$. Even for a high value of the mass loss rate $\dot{M}_{-4} = \dot{M}/(10^{-4} M_\odot yr^{-1}) = 1$, the density is orders of magnitudes lower than that required to produce the observed line flux. Weth et al [9] argued that high density clouds could

be produced from a low-density and low-velocity wind, but it remains to be assessed how those clouds could be accelerated to high velocities. Alternatively, nearly all the formation scenarios of GRB progenitors involve substantial mass loss when the system is in a common–envelope phase, a process which is likely to form a disk[2]. Interaction of the expanding shell of the GRB with the disk could produce a shock-heated gas with density and velocity of the same order of magnitude as needed here [10]. The emission from this region can be represented by pure thermal plasma, i.e. in thermal and collisional ionization equilibrium, but in this case emission from a recombination edge is negligible [10]. In fact, to effectively ionize iron atoms, electrons should have a temperature comparable to the edge energy, therefore producing a feature too smeared to be detected. This may be circumvented if the electron population of the shock-heated plasma does not reach complete equilibrium, but the conditions under which this happens have yet to be studied. The simplest explanation of our results is a mass ejection by the progenitor with the same velocity implied by the observed line width. The ejection should have then occurred $\approx R/v =$ (i.e., a few months) before the GRB.

The distribution of ejecta and the GRB emission are not highly anisotropic. Let $\Delta\Omega$ be the solid angle of the medium illuminated by the GRB and ΔR its size. The mass contained in the line emitting volume is $M = \Delta\Omega R^2 \Delta R n m_p$. Substituting the limit of the mass derived in the left hand side of eq(1) and the limits $\tau = \Delta R n \sigma_T < 1$ and $\xi > 10^4$ we derive

$\Delta\Omega/4\pi \gtrsim 60 X_{Fe}^{-1} > 0.1$

where the lower limit corresponds to the extreme case of ejecta of pure iron. The GRB emission and the distribution of the medium around it cannot therefore deviate substantially from isotropy. The lower limit we have derived on the beaming factor [3] is marginally compatible with the estimate of [20]. We note, however, that our results refer to the emission

[2]The commom–envelope phase happens when the hydrogen envelop of the secondary star expands engulfing the compact primary (neutron star or black hole). Friction and tidal forces cause the compact object to spiral in the giant's core, ejecting the hydrogen envelope preferentially along the orbital plane, forming a disk [28]

[3]The beaming factor $\Delta\Omega/4/\pi$ is the fraction of sky over which GRB photons are emitted. It is equal to 1 if the emission is isotropical and $\approx \theta^2/4$ in the case of a jet with opening angle θ

inside the line emitting region while the measurements mentioned above are based on the appearence of a break in the light curve 2-5 days after the GRB, i.e., when the fireball has overcome the line region. It is then possible that the initial GRB emission is isotropic and it is then collimated by the interaction with a funnel-like medium. This limit on anisotropy allows the determination of the total, isotropic, electromagnetic energy produced by a GRB, which for GRB991216 is $E > 7.2 \times 10^{52}$erg $s^{-1} = 0.04 M_{\odot} c^2$. Another important implication of the previous limit is on the iron abundance of the medium, that has to be much higher than solar ($X_{Fe} > 60$). This high value of the iron abundance indicates that the ejecta were - at some stage of the progenitor evolution - produced by a supernova explosion [29, 30].

In conclusion, the most straightforward scenario that emerges from all the pieces of evidence we have gathered is the following. A massive progenitor - like a hypernova or a collapsar [31, 32] - ejects, shortly before the GRB, a substantial fraction of its mass. This event is similar to a supernova explosion, like in the case of the SupraNova model [33].

References

[1] Fryer C. L., Woosley S. E. & Hartman D. H. *Astrophys. J.* , **526**, 152 (1999).

[2] Mészáros P. & Rees M. J., *Mon. Not. R. Astr. Soc.* , **299**, L10. (1998)

[3] Boettcher M., Dermer C.D.D., Crider A. W. & Liang E. D. *Astron. Astrophys.* , **343**, 111, (1999).

[4] Perna R. & Loeb A., *Astrophys. J.* , **501**, 467 (1998).

[5] Wijers R.A.M.J. & Galama T.J., *Astrophys. J.* , **523**, 177 (1999)

[6] Sari R., Piran T., & Narayan R. *Astrophys. J.* , 497, L17 (1998).

[7] Lazzati D., Ghisellini G. & Campana S., *Mon. Not. R. Astr. Soc.* , **304**, L31 (1999).

[8] Vietri M., Perola G.C., Piro L. & Stella L., **308**, L29 (2000).

[9] Weth C., Meszaros P., Kallman T., Rees M., *Astrophys. J.* **534**, 581 (2000).

[10] Boettcher M. & Fryer C.L., *Astrophys. J.* , submitted, preprint available at http://xxx.lanl.gov/abs/astro-ph/ astro-ph/0006076.

[11] Piro L. *et al. Astrophys. J.* , **514**, L73 (1999).

[12] Yoshida A. *et al.* , *Proc. of Gamma-ray bursts in the afterglow era* (eds F. Frontera and L. Piro) (*A&AS***138**, 433 (1999).

[13] Daisuke Y. *et al. Publs. Astron. Soc. Japan* , **52**, (2000).

[14] Kulkarni S. R. *et al. Proc. of 5th Huntsville GRB Symposium*, in press (astro-ph/0002168) (2000).

[15] Weisskopf, M. C. , O'Dell, S. & van Speybroeck, L. P. *Proc of Multilayer and Grazing Incidence X-Ray/EUV Optics III* (eds R. B. Hoover and A. B. Walker), 2 (SPIE, 2805, 1996).

[16] Kippen R.M., R.D. Preece, & T. Giblin, GCN n.463 & n. 504 (2000).

[17] Takeshima T., Markwardt C., Marshall F., Giblin T. & Kippen R.M., GCN n. 478 (2000).

[18] Hurley K. *et al.* GCN n.484 & 505 (2000).

[19] Piro L., Garmire G., Garcia M. & the CXC team, Marshall F., Takeshima T. , GCN n. 500 (2000).

[20] Halpern J.P., *et al. Astrophys. J.* in press, preprint available at http://xxx.lanl.gov/abs/astro-ph0006206 (2000).

[21] Frail D. A., *et al. Astrophys. J.* in press, preprint available at http://xxx.lanl.gov/abs/astro-ph/0003138 (2000).

[22] Piro L. *Proc. of UV and X-ray spectroscopy of laboratory and astrophysical plasmas* (eds E. Silver and S. Kahn) 448 (Cambridge Univ. Press, Cambridge 1993).

[23] Paerels F., E. Kuulkers, J. Heise, J. in 't Zand, D. Liedahl, *Astrophys. J.* in press, preprint available at http://xxx.lanl.gov/abs/astro-ph/0004188 (2000).

[24] Amati L. *et al.* , Science, this issue.

[25] Kallmann T. R. & McCray R. *Astrophys. J. Suppl. Ser.* , **50**, 263 (1983).

[26] Vreeswijk P.M. *et al.* GCN n. 496, (2000).

[27] Djorgovski S. G. *et al.* GCN n. 510 (2000).

[28] Sandquist, E., Taam, R.E., Chen, X., Bodenheimer, P., & Burkert, A. *Astrophys. J.* , **500**, 909 (1998).

[29] Woosley S. E., & Weaver T.A. *Astrophys. J. Suppl. Ser.* , **101**, 181 (1995).

[30] Bouchet P. *et al. Astron. Astrophys.* , **245**, 490 (1991).

[31] Paczynski, B. *Astrophys. J.* , **494**, L45 (1998).

[32] Woosley S. E. *Astrophys. J.* , **405**, 273 (1993).

[33] Vietri M. & Stella L., *Astrophys. J.* , **507**, L45 (1998).

[34] See Chandra calibration reports in http://asc.harvard.edu/cal

[35] We thank the Chandra team for the support, in particular F. Nicastro and A. Fruscione for the help in data reduction. We thank for M. Boettcher for his critical suggestions. We acknowledge useful discussions on the observational strategy with G. Ricker and L.A. Antonelli for comments. MG acknowledges the support of NASA Contract NAS8-39073 to the CXC.

Figure 1 The X-ray afterglow spectrum of GRB991216 obtained with the Chandra high-energy gratings (High Energy (HE) and Medium Energy (ME) summed together. The background is negligible. The exposure time of the observation was 9700 s. In order to increase the statistics, the grating spectrum has a bin size of 0.25 Å, including about 10 resolution elements of the ME and 20 of the HE. The dashed line represents the best fit power law on the the 0th order ACIS-S spectrum. The peak (i.e. 2 bins) around 3.5 Å(E=3.5 keV) is detected with 4.7 σ confidence. We have verified the robustness of the detection against the continuum level. The significance remains above 4σ even when assuming a worst case systematic uncertainty in the cross-calibration of the two instruments of 15% [34]. In the inset the region on the line is shown with a finer binning. The dotted line represents the best fit continuum model to the 0th order ACIS-S spectrum after the addition of a recombination edge in emission (see Fig.2). The line parameters (errors on best fit parameters correspond to 90% confidence level for 1 parameter of interest) are $I_L = (3.2 \pm 0.8)\ 10^{-5}\mathrm{cm}^{-2}\ \mathrm{s}^{-1}$ $E.W. = (0.5 \pm .013)$ keV, width(σ_L)=(0.23 ± 0.07) keV, $E = (3.49 \pm 0.06)$ keV. The spectrum has been examined at higher resolution to confirm the line broadening. Since each of the spectral bins in the figure includes several resolution elements of the instrument, a narrow feature would appear in no more than 1 single bin, regardless of how fine is the binning, while this is not the case. Deviations around 7 $\mathring{A}$ are $\approx 3\sigma$, and it is worth noticing that they are close to the expected energy (at z=1.0) of the recombination edge of hydrogen-like Sulphur. Deviations at $\approx 4.4\ \mathring{A}$ are less than 3 σ.

Figure 2 The X-ray afterglow spectrum of GRB991216 obtained with the Chandra ACIS-S (0th order). The energy resolution of ACIS-S is 0.1 keV (FWHM) at 4 keV and the background is negligible on the whole energy range. The better response at high energies compared to the gratings allows us to single out the presence of a further emission feature. Fitting a model (continuous green line) composed by an emission edge (blue dashed line) plus a power law (green dashed line) plus line (orange dashed line) provides a satisfactory fit to the data ($\chi^2_\nu = 0.95$, $\nu = 26$). The addition of the edge improves the fit by $\Delta\chi^2/\chi^2_\nu = 16.3$,

that corresponds to a confidence level of 99.5% (F test). Best fit parameters of the edge are $E = 4.4 \pm 0.5$ keV, $I_{edge} = (3.8 \pm 2.0)\ 10^{-5}$cm^{-2} s^{-1} and width $\sigma_{edge} > 1$ keV. For the power law we derive ($F_X(2-10keV) = 2.3\ 10^{-12}$erg cm^{-2} s^{-1}, photon index $\Gamma = 2.2 \pm 0.2$, $N_H = (0.35 \pm 0.15)\ 10^{22}$ cm^{-2}, consistent with the absorption in our Galaxy ($N_{HG} = 0.21\ 10^{22} cm^{-2}$). Line parameters are consistent with those derived from the grating. Moreover, the edge is consistent with the grating data, as shown by the dotted line in the inset of Fig.1.

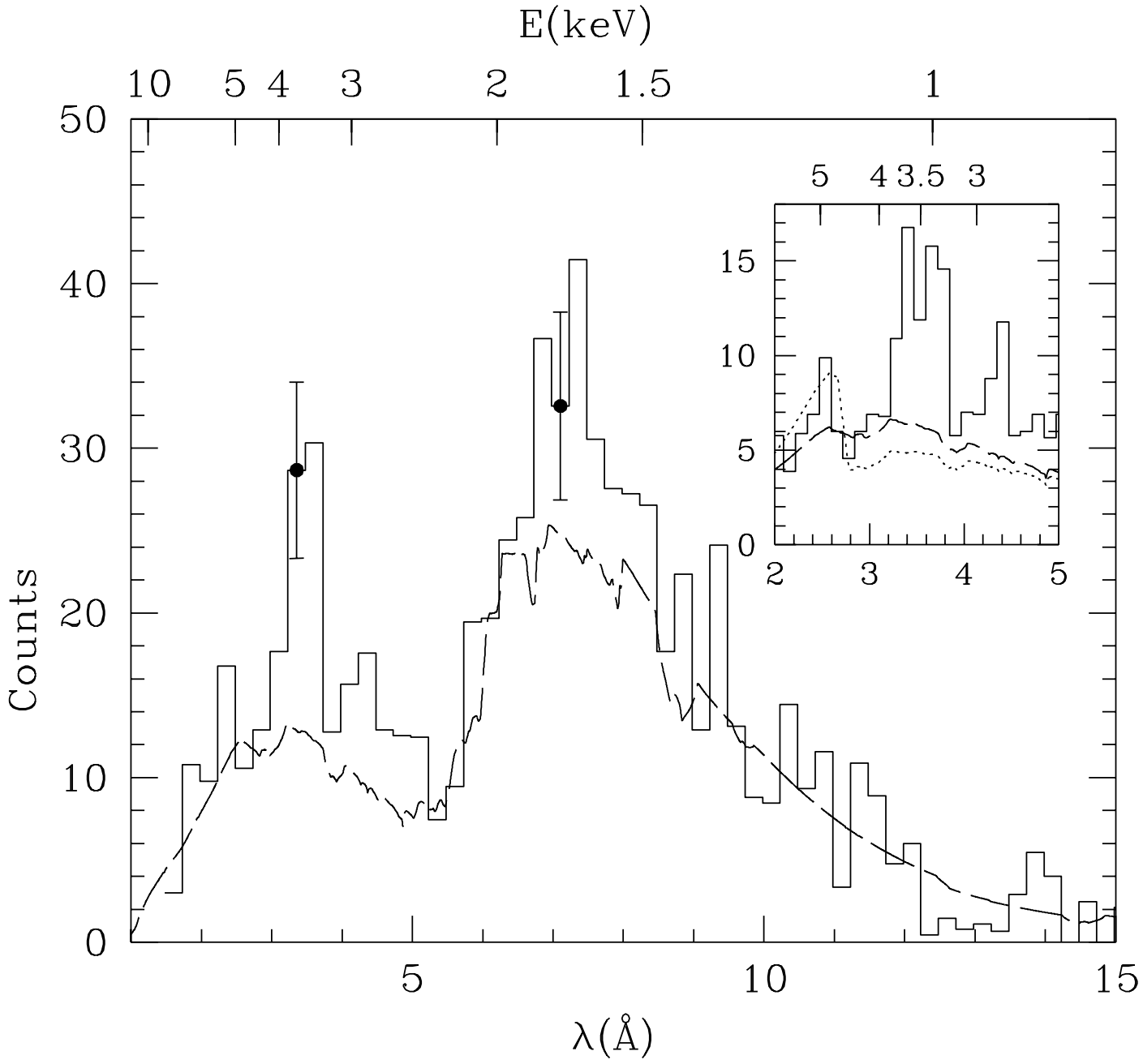
E(keV)
10
5
4
3
2
1.5
1
50
40
30
20
10
0
Counts
5
10
15
λ(Å)
5
4
3.5
3
15
10
5
0
2
3
4
5

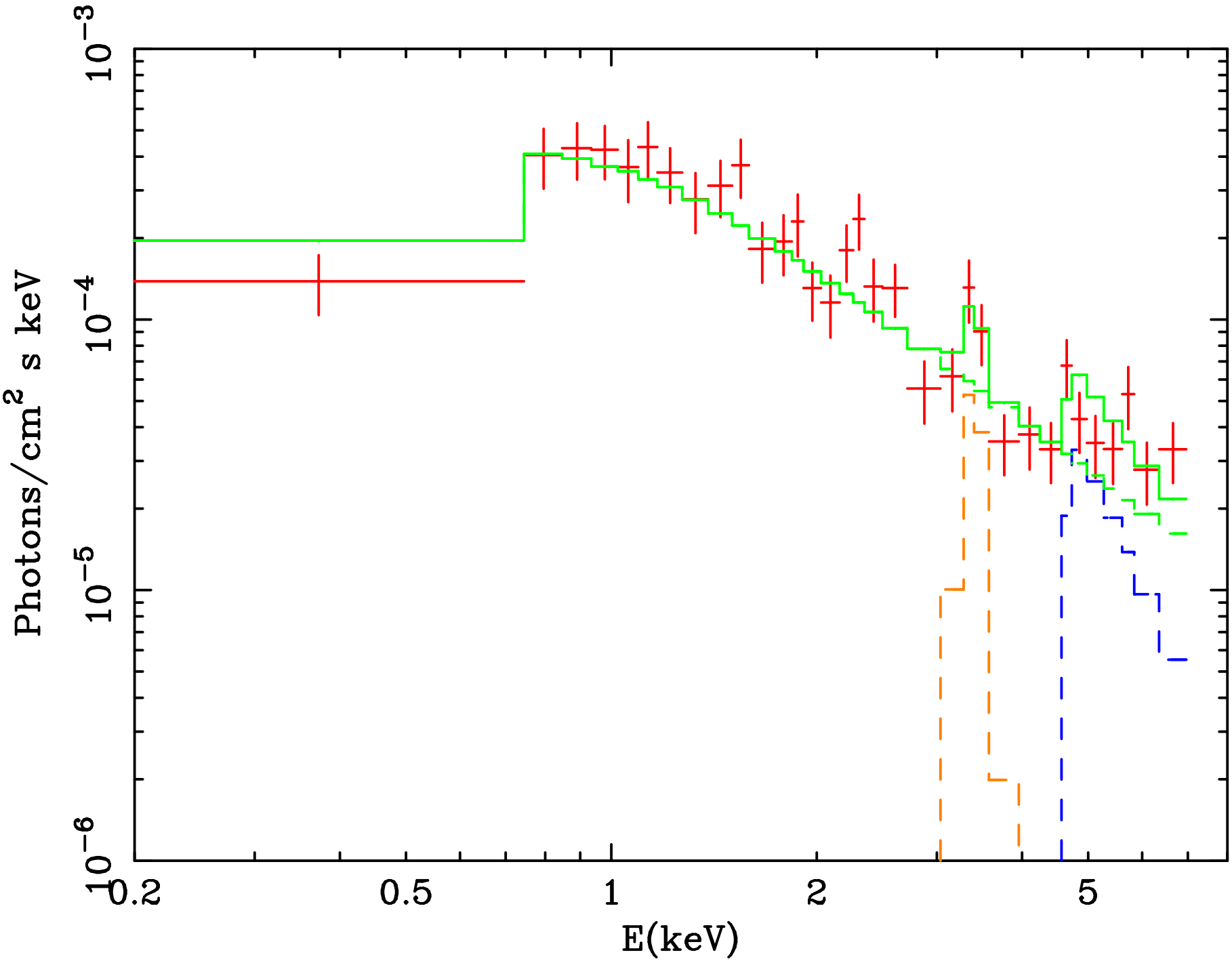
Photons/cm^2 s keV
10^{-3}
10^{-4}
10^{-5}
10^{-6}
0.2
0.5
1
2
5
E(keV)